

Radiation Effects in Silicon

Peter Voss

1. Introduction

Any silicon device that has left the manufacturing process and goes into an application will be exposed to some degree of high-energy electromagnetic or particle radiation. Most devices, however, have seen the highest degree of exposure to particle irradiation already during the manufacturing process, the most common irradiation process being ion implantation. Less common is the exposure of silicon intended for the manufacture of high-voltage power devices to high fluences of low-energy neutrons for the purpose of neutron transmutation doping and these bipolar devices may also have been exposed to the various methods using high-energy electrons, protons, alpha particles and gamma rays to adjust carrier lifetimes or doping levels. These methods will be described in this section.

Most applications of silicon devices take place at ground level where the devices are exposed to a low rate background radiation originating from radioactive materials in the device or in the package or from cosmic rays. A sizable number of devices is used in airplanes which during flight are exposed to a level of cosmic ray radiation about 300 times that at ground level and some devices are operated in space environments or close to particle accelerators where the radiation level can be quite high and can lead to degradation or various upsets of the devices. We will also look into these aspects of device irradiation.

2. Interaction of radiation with silicon

Depending on whether the interaction of a silicon device with radiation occurs already during the manufacturing stage or during its application, different aspects of the interaction are of interest. During the manufacturing process it is predominantly the incorporation of ions as dopants or the generation of crystal defects that act either as recombination centers or as dopants, while during application the focus is on the charge generated by single particles - either by the particle itself or as secondary charge after a nuclear reaction -, or the focus is on the long term degradation and doping effects after high-fluence exposures which then are often similar to those effects employed during manufacturing in a prescribed way. Naturally, the ions used in the manufacturing process and the particles encountered by a device during application are seldom of the same kind. There is often also a significant difference in the energies the particles or the electromagnetic radiation possess. Ion implantation energies are typically in the keV range. Energies for the intentional introduction of damage are typically of the order of a few MeV, while the energies of cosmic ray particles reach into the GeV range and way beyond.

When high-energy particles are used for processing silicon, the main interest is in an exact determination of the dosage, in obtaining the right penetration depth and in the annealing procedures for undesired crystal defects. When particles can interact with the finished device in an application, one has to find ways to determine the probability for single event effects (SEE) due to the charge or the damage generated during a specific operation mode. When the finished device is exposed to continuous high fluxes of radiation, there is usually no possibility to at least partially anneal the generated defects in regular cycles, though there are applications where this is the only way to guarantee long term operation.

Tab. 1 lists a number of typical effects of the various types of radiation.

<p>silicon bulk</p> <p>carrier generation</p> <p>charge collection at pn-junctions</p> <p><u>detectors, normal operation</u></p> <p><u>low-voltage devices, single event effects (SEE)</u></p> <p>Single Event Upset, Soft Error (SEU, SER)</p> <p>latchup → thermal breakdown, Single Effect Burnout (SEB)</p> <p><u>high-voltage devices, current bursts (Single Effect Burnout)</u></p> <p>carrier multiplication → immediate burnout</p> <p>transistor amplification → second breakdown, delayed burnout</p> <p>damage</p> <p>recombination centers</p> <p><u>dark current generation</u></p> <p><i>detectors, power devices, capacitors (retention time)</i></p> <p><u>low injection carrier lifetime</u></p> <p><i>bipolar devices turnoff</i></p> <p><u>high injection carrier lifetime</u></p> <p><i>bipolar devices forward voltage drop</i></p> <p>traps</p> <p><u>collection efficiency of detectors</u></p> <p>doping centers</p> <p><u>p-doping</u></p> <p><i>detectors, change of operating conditions</i></p> <p><i>power devices, drift of blocking voltage</i></p> <p><u>n-doping (protons)</u></p> <p><i>power devices, drift of blocking voltage</i></p> <p>silicon oxide</p> <p>carrier generation</p> <p><u>oxide charge, surface charge</u> → gate voltage drift</p> <p>damage</p> <p><u>reduction of maximum tolerable fieldstrength</u>, → Single Event Gate Rupture (SEGR)</p> <p><u>leakage, loss of charge</u></p>

Tab. 1 Various effects of radiation in silicon and silicon oxide

The reasons for deteriorations and upsets of silicon devices fall into a few basic categories, but the consequences are very widespread.

The most elementary effect is the generation of charge in the silicon bulk by the absorbed particle. In a detector the charge gives rise to the current pulse to be analyzed. In this case an undisturbed signal with high collection efficiency is desired. Similar current pulses occur in any circuit that has a charge collecting capability. Depending on how the collecting cell is interconnected with neighboring cells the current pulse can lead to upsets. The details depend on the current shape, operating voltage etc.. In the capacitor cell of a memory device it is the change in the charge of the cell itself that may flip its logic state. In arrangements with simple pn-junctions or in surface counter arrangements the local disturbance of the field distribution can cause avalanche multiplication and possible destruction. In multilayered structures there may be parasitic transistors incorporated that react to a primary current pulse and cause latchup of a device or device cell and in unfavorable situations may lead to destructive second breakdown due to thermal runaway.

Finally there is the effect of the generated lattice defects that in bipolar devices cause a change in carrier lifetime. Often the concurrent increase in dark current through the radiation-induced recombination centers is of equal or even more concern.

When the particle is absorbed in an insulating layer of silicon oxide or silicon nitride, most of this charge is trapped in the layer or at its surface. It can be moved either through high electric fields or dissipated through elevated temperatures. In MOS devices the changes resulting from the trapped charge normally have detrimental effects, e.g. when the gate voltage changes, but such

change can also be taken advantage of in dosimeters. When the movement of the generated charge takes place immediately after generation, it may result in oxide breakdown, i.e. in gate rupture.

2.1. Particles

2.1.1. Protons, alpha-particles, heavy ions

The status of the ways to determine the stopping of high-energy particles in solids is reviewed in [1]. Ziegler and Biersack developed a program, TRIM or SRIM [2], for calculating the stopping and range of ions in solids. Some examples are given in Fig. 1. The energy transfer or stopping power is given versus penetration depth. For clarity, energy transfer is presented here in units of keV/ μm , whereas it is usually plotted as MeV/ mg/cm^2 . The scaling factor is $1 \text{ keV}/\mu\text{m} = 4.31 \text{ keV}/\text{mg}/\text{cm}^2$. All these examples are for energies in the MeV range, i.e. significantly higher than used for ion implantation. The curves for protons and alpha particles are examples for energies used for lifetime adjustment or for energies of particles originating from radioactivity or cosmic rays. The curve pertaining to silicon ion energy of 30 MeV is an example for a high energy recoil of a nuclear reaction which might result from a collision of a high-energy neutron with a silicon nucleus. The 200 MeV curve is shown to demonstrate the different shapes of the stopping power curves. Stopping power is usually abbreviated as LET for 'Linear Energy Transfer', which is obviously not a good description for the lighter particles.

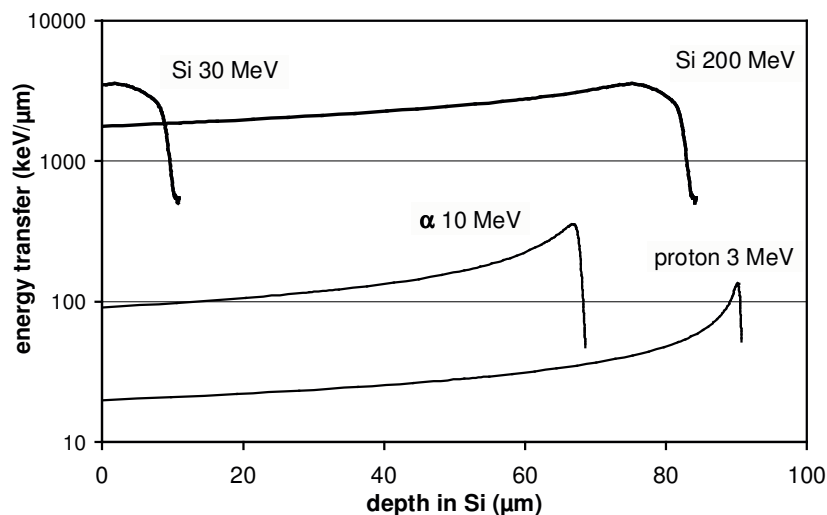


Fig. 1 Stopping power of protons, alpha particles and silicon ions in silicon calculated with TRIM [2]

The interaction of the ions causes displacement of the recoil atoms of the target and gives rise to interstitial atoms and lattice vacancies. Interstitials and vacancies have a high mobility even at room temperature and become less mobile by forming complexes or by attaching to dopants in the silicon, in the bulk first of all to carbon or oxygen which are usually present at concentrations around 10^{15} cm^{-3} , or in case of oxygen even higher. It appears that the vacancy reactions are particularly important. Table 2 shows a number of possible combinations.

vacancy reactions
$V + V \rightarrow V_2$
$V + V_2 \rightarrow V_3$
$V + O \rightarrow VO$
$V + VO \rightarrow V_2O$
$V + P \rightarrow VP$

Tab. 2 Radiation damage vacancy reactions, from [3]

Of these reaction products the divacancy and the vacancy-oxygen complex are effective as recombination centers, whereas the divacancy-oxygen complex forms an acceptor level. The effectiveness in one or the other way depends on the position of the level in the band gap, on the capture cross section for electrons and holes and on the position of the Fermi-level. For details see for example Baliga [4]. Recombination processes for the low and the high injection case can generally be described on the basis of the Shockley-Read-Hall model [4] with one or several single-level recombination centers. This approach apparently has failed for the modeling of dark currents when the damage is generated by high-energy particles, where it results in current levels that are two orders of magnitude too low [5]. The observed high dark current levels are assumed to be caused by the overlap of recombination levels generated in damage clusters [6].

In the normal implantation process for doping purposes all damage is annealed as much as possible, whereas when radiation is used for trimming of device properties one obviously wants to retain at least some of the generated defects or complexes. In these cases one main aspect of the treatment after implantation is that the finished device has to have stable electrical properties in the range of application. For many high-voltage power devices the maximum application temperature reaches only up to 125 °C or 140 °C. In such cases an annealing process at a temperature of 250 °C over several hours has proved to be sufficient. Most defects can be annealed at temperatures around 350 °C, but - depending on the preprocessing - defects can be stable well beyond a temperature of 450 °C.

Implantation of protons or helium ions is predominantly used in order to adjust carrier lifetime in bipolar devices. As can be seen from Fig. 1, using protons has the advantage that the energy transfer is highly localized in the region where the proton comes to rest and therefore almost all the damage is generated there. As can be seen in Fig. 1 to a lesser degree this also holds true for helium ions. In this way one can insert regions of increased local carrier recombination rate. For some applications proton implantation has the disadvantage that when a high dosage is required the implanted hydrogen causes a n-doping that may affect the breakdown voltage of the treated device in an undesired fashion [7]. Naturally, this behavior can also be used as an additional process tool in some instances. Helium ions and any heavier ions cause p-doping via the V_2O -center, but in case of helium at a much lower generation rate as compared to protons.

2.1.2. Electrons

In comparison to heavier particles, electrons have a much higher penetration depth and are therefore well suited when uniform generation of damage is required. Electron irradiation has become a standard method for the adjustment of the carrier lifetime in large area power devices like diodes and thyristors. These device often have very stringent requirement with regard to their blocking behavior, which in case of thyristors is governed by dark current generation in the space charge region and the low injection carrier lifetime outside of it. The dynamic behavior of these devices during turn-off as a trade-off with respect to the forward conducting behavior is governed by the carrier lifetimes for high and low injection.

Electron irradiation has to a large extent replaced conventional diffusion methods of lifetime control like doping with gold or platinum. This is largely due to the convenience of being able to do an exact lifetime trimming, but for high-voltage devices also to a large extent because of the requirement for the blocking current to be as low as possible. For some medium-voltage devices for which the dynamic properties are often most critical, it is still not unusual to combine conventional diffusion techniques and radiation techniques to achieve optimum properties for the carrier lifetime.

Work on electron irradiation started with electrons having energies below 2 MeV and did not look very promising when the results were compared with gold diffusion. Similar unpromising results were obtained with gamma rays (the highest transfer energy to electrons is 1.1 MeV). It was only after it was shown that higher electron energies yield a better trade-off that electron irradiation became widely used. Fig. 2 shows the results of the first investigation of the influence of the electron energy [8].

Originally it was thought that the divacancy was the main generated recombination center, but currently there are indications that the VO center (A-center) is dominant. This is supported by the fact that lifetime measurements on electron irradiated unprocessed float-zone silicon wafers (oxygen content $< 1 \cdot 10^{15} \text{ cm}^3$) have indicated drastically reduced generation rates for the recombination centers.

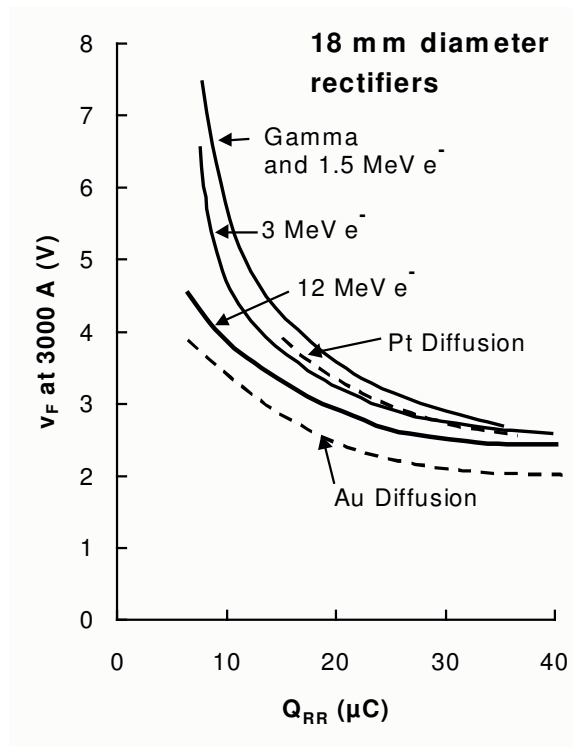


Fig. 2 Forward voltage drop versus reverse recovery current for diodes irradiated with gamma rays or electrons as compared to diodes diffused with platinum or gold [8]

2.1.3. Neutrons

Neutrons are considered here because they are the main contributors to single event effects at ground level. They are generated in particle showers that occur when high-energy particles hit the outer atmosphere of the earth. Due to their electrical neutrality neutrons will not interact with the electron gas as protons do and therefore they have a larger penetration depth in matter than the latter. Interaction takes place solely with the atomic nuclei. At energies above approximately 100 MeV the stopping mechanism for neutrons and protons becomes similar. This is an important feature when it comes to testing devices for cosmic ray failure rates.

2.2. Nuclear reactions

When solids are irradiated with particles, nuclear reactions with the target set in at approximately 1 MeV/amu particle energy, where amu stands for atomic mass unit. During device processing this is a side effect that may deserve some attention because of the resulting radioactivity. On the other hand, nuclear reactions are the major cause for single event effects at ground level and in the atmosphere. Single event upsets in signal processing devices are first of all due to the charge generated per unit volume. Experimental experience shows that the charge generated by a proton

is usually not sufficient to cause an upset, whereas the denser charge tracks of helium ions (compare Fig. 1) originating from packaging material polluted with minute traces of alpha emitters were historically the first obvious causes for upsets at ground level. Any particle heavier than helium can cause upsets. Heavier nuclei are generated when a primary particle, e.g. a high-energy neutron or proton, collides with a silicon atom. This results in a large variety of fission products, light fractions like alpha particles and

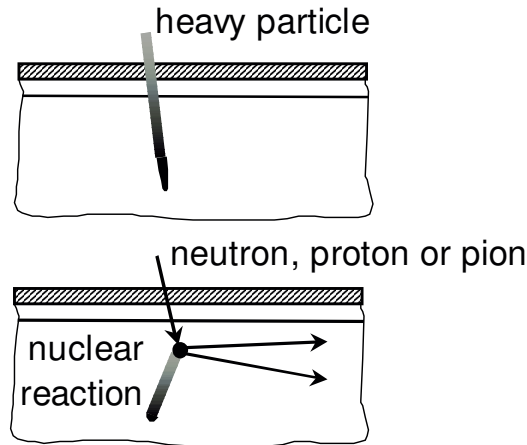


Fig. 3 Schematical representation of heavy ion or lighter particles being absorbed in a metallized junction device

Residual Nucleus	Type	MeV	Residual Nucleus	Type	MeV
$^{12}\text{C}^6$	12, 6	8,15	$^{27}\text{Al}^{13}$	27, 13	2,73
	p	1,26		p	84,07
	n	44,07		p	52,82
	n	12,42	$^{26}\text{Al}^{13}$	26, 13	0,18
	n	16,90		n	134,88
	n	3,34		n	3,08
	alpha	11,04		n	1,71
	alpha	3,57			
	alpha	4,12			

Tab. 3 Examples of spallation events with 150 MeV protons incident on silicon [10]

heavier fractions, in the case of silicon predominantly ranging from carbon to silicon. Tab. 3 shows selected results from calculations of Tang using the simulator NUSPA[9] of spallation products from nuclear events after collisions of 150 MeV protons with silicon [10], indicating the diversity of the secondary products and of their energies. Recoiling Si atoms constitute the largest fraction at low energies, whereas there is a considerable amount of high-energy oxygen and carbon atoms with energies reaching up to about 30 MeV.

In integrated memory and logic devices the unit cells are small and therefore not all the generated charge may be deposited in the cell where the reaction occurs. Depending on the flight path of the secondary particles several cells may be affected, leading to multiple upsets. For these devices the generated charge is of main concern. However, in charge storing junctions the damage may lead to an increase in dark current to such a degree that the retention time is strongly reduced and that in extreme cases the stored information is lost.

Depending on the design of the cell, a relatively large amount of charge may be collected due to diffusion or due to a distortion of the space charge region by the ion track, leading to charge funneling [11]. The distortion of the space charge region by the ion track can cause drastic results in high-voltage power devices when it initiates avalanche carrier multiplication. Schematical representations of space charge region distortions are depicted in Fig. 4.

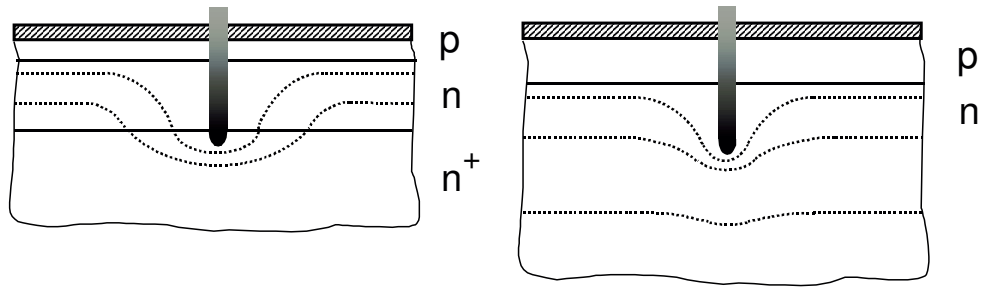


Fig. 4 Schematical representation of the effect of ion tracks in a low-voltage and in a high-voltage device. Dashed lines indicate equal potential lines. In the low-voltage device the space charge region expands into the highly doped substrate and may no longer be able to support the original voltage. Charge generated in the substrate will be collected at the junction (funneling). In the high-voltage device the space charge region also expands. The fieldstrength at the tip of the ion track may become so high that carrier multiplication sets in.

3. Radiation sources

3.1. Natural radiation background

The first single event effects in silicon devices that could be traced to their origin were caused by alpha particles emanated by the packaging material or by the metallization [12,13]. These causes have been reduced to a large extend, but are by no means completely eliminated. The main natural radiation background affecting silicon devices originates from cosmic rays.

In outer space protons are most abundant, largely as part of the solar wind with energies into the MeV range, whereas protons from deeper space can have energies as high 10^{20} eV. Cosmic rays also contain heavier ions, mainly iron.

The earth atmosphere shields most of this radiation. High-energy particles penetrating the earth's outer atmosphere lose their energy through nuclear reactions with the air molecules and cause showers of secondary particles. The atmosphere of the earth provides a shielding of about

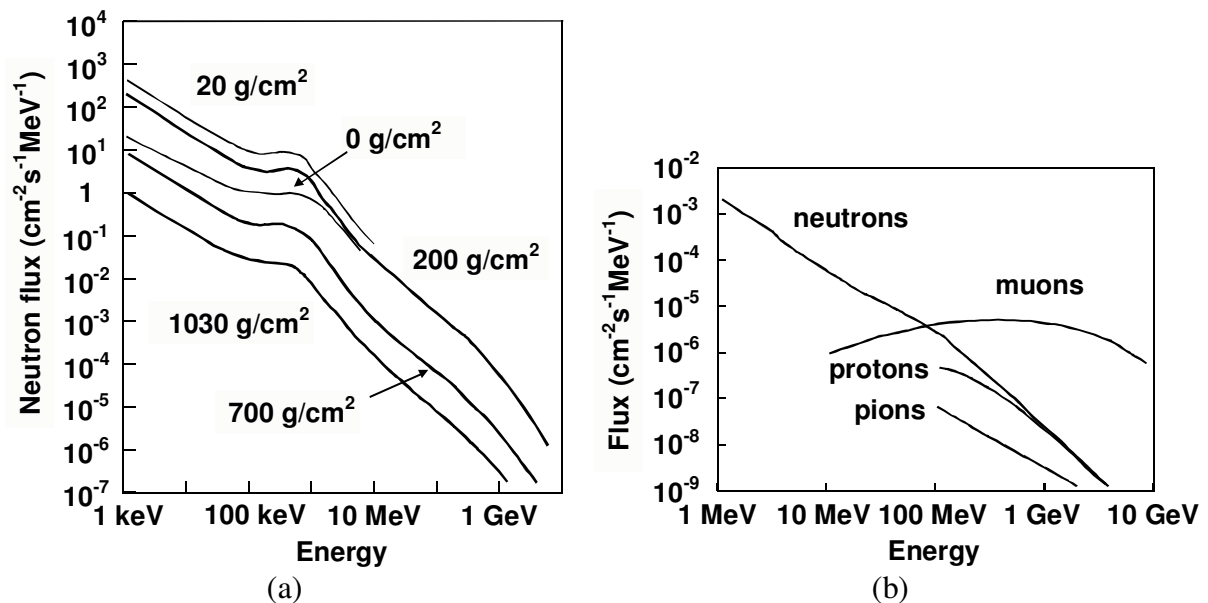


Fig. 5a Neutron flux vs. altitude. 1030 g/cm² corresponds to sea level, 200 g/cm² to a height of 10 km, i.e. to airplane cruising level. Detail from [14].

Fig.5b Theoretical curves of flux of cosmic rays at New York City. From [14].

1 kg/cm². For the secondary particles to reach ground level, the energy of a primary proton has to be of the order of 1 GeV. Since the energy of the primary particle can be much higher, the energies of the secondary particles in the shower can reach beyond 1 GeV (Fig. 5b). Due to the influence of the solar wind on the earth's magnetic shielding, cosmic radiation at ground level is actually reduced in times of increased solar activity.

The highest density of particles is reached at a height of about 18 km above ground (Pfozter peak). Fig. 5a shows a plot of the neutron flux versus energy for different heights [14]. The way this diagram is plotted on a logarithmic scale, a one decade decrease of neutron flux of per decade of energy means equal numbers of incident particles per decade energy. Fig. 5b depicts the flux at ground level [14]. At high energies muons dominate, but since these have a very low absorption coefficient they play a very minor role with respect to upsets as compared to the other particles. At ground level neutrons cause most interactions.

3.2. Exposure to radiation during operation

The natural radiation background is of concern for a number of failure modes. Some of these failures may just be a nuisance to the end user, others lead to total failure of a piece of equipment and some may even endanger human life when they occur in the electronics of defibrillators or of pacemakers.

Deterioration of device properties, upsets and failures were naturally first encountered with devices operated in highly ionizing environments, e.g. when they were used as radiation detectors or in space applications. The airplane industry was next to realize this problem and only fairly recently has it become obvious that cosmic rays can be a rather serious problem at ground level, in particular for power devices.

Silicon devices are increasingly used as radiation detectors in accelerator facilities under conditions where they are exposed to extreme rates of radiation.

Electronics operated in space are exposed to high levels of radiation in the radiation belts of the earth or other planets and during bursts of the solar wind. The spacecraft community has learned to live with this problem, since it is unavoidable. Spacecraft can be shielded to some degree against heavy particles and partly also against the lower energy lighter particles consisting mostly of protons. Special device designs enable radiation-hardened features. Error detection and correction codes (EDACs) eliminate most if not all bit losses in digital equipment. But as more electronic parts are used in spacecraft, e.g. as hydraulically operated parts are replaced by power electronics, new failure modes surface. Some of these are modes of total failure, so that the question of tolerable levels for total failure is becoming more important. A general tendency for all devices seems to be an attempt to use commercial (COTS - Commercial Off The Shelf) parts as much as possible instead of special hardened designs, because the performance of the latter is often several generations behind that of state-of-the-art parts.

3.3. Prediction of SEEs

For any kind of application in a radiation environment it is essential to have an understanding of the upset and failure rates to be expected. The prediction of SEE events can be relatively simple for devices like diodes operated at ground level, where, e.g. a test with neutrons or protons at one energy gives results that can be directly matched with reference results. On the other hand, predictions can become very complicated when complex electronics parts, the details of which are often unknown to the user, are used in space under constantly changing radiation conditions. Several codes have been developed for SEE prediction by manufacturers and users. These incorporate either all the details of the nuclear events and of the circuitry of the device for performing Monte Carlo calculations or they are based on accelerator testing of basic structures

or complete devices under various conditions with respect to particles, particle energies, irradiation angles and device operation conditions. Details are given in [15], [16], [10] and [17].

3.4. Accelerators

For the various methods of irradiation treatment and for accelerated tests of various failure modes a variety of accelerators is required.

High-energy electron accelerators used to be relatively rare, but lately there has been a proliferation of new industrial facilities with the capability to scan large areas. These installations have typical energies of the order of 10 MeV.

The requirements for other particle accelerators depend on whether they are needed for processing or for testing. Processing as treated here does not include standard ion implantation methods, i.e. it refers mainly to proton and helium implantation. A proton implantation of 50 μm requires an energy of about 2 MeV (see Fig.1). Such energies can be achieved with tandem van-de-Graaf or dynamitron machines.

For tests that try to reproduce cosmic ray conditions larger facilities are needed. A number of accelerators are available for routine testing with protons, neutrons and heavy ions. Proton energies reach up to 1 GeV. A survey is given in [18]. Testing in these installations is rather costly and therefore one tries to keep these test at a minimum.

4. Device exposure to ionizing radiation

4.1. Adjusting device parameters

Radiation as a means to adjust device parameters is mainly used with high-power bipolar devices. As already shown in the example of Fig. 2, one wants to achieve the optimum trade-off for these devices between forward voltage and dynamic properties like reverse recovery charge or turn-off time or one intends to optimize for a specific turn-off behavior with respect to the way the current flow ceases during turn-off. Electron irradiation with energies above 4 MeV in many cases has proved to provide a good compromise with respect to low dark current levels and low carrier lifetimes under low and high injection conditions [4]. This applies first of all to thyristors that have symmetric blocking characteristics in forward and reverse direction where any unsymmetric type of irradiation usually causes a strong deterioration in one direction. Assuming that the generation of recombination centers is proportional to the dosage, it is generally assumed [19] that the change in carrier lifetime follows the law

$$1/\tau = 1/\tau_0 + \text{const} * \text{dosage}$$

where τ_0 is the carrier lifetime before irradiation. The damage constant is strongly dependent on the processing history of the device, in particular on the level of oxygen doping. Usually carrier lifetime cannot easily be determined directly and therefore similar relations are used for the reverse recovery charge (Q_r) or the turn-off time (t_q). Since the relation between these properties and carrier lifetime depends on measurement conditions and device design, such assumptions usually hold only over a narrow range. Usually $1/Q_r$ and $1/t_q$ increase more than proportionally with dosage.

For asymmetric devices like diodes, proton or helium irradiation offers an additional degree of freedom, since the carrier lifetime can be reduced locally (see Fig. 1). This has proved to be very useful for the adjustment of the turn-off behavior of diodes for which a 'soft' turn-off behavior is often desired, as a contrast to a 'hard' turn-off or 'snap-off' behavior that may lead to a destruction of the device or to undesirable circuit ringing (Fig.6). With the local lifetime control one can

generate pockets with higher carrier lifetime serving as carrier reservoirs which supply the carriers for the soft current tail part [20].

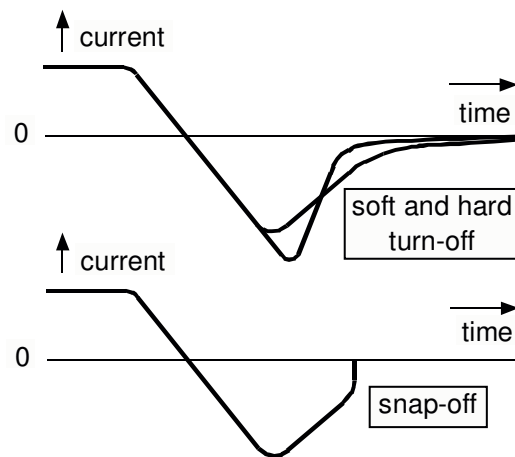


Fig. 6 Schematics of various diode current transients during turn-off

In these applications the n-doping effect of implanted protons is sometimes detrimental, and therefore helium is preferred for which a p-doping occurs only at much higher doses. However, in cases where the local breakdown voltage of a device is to be adjusted, the n-doping as well as the p-doping effects of protons and of helium ion damage, respectively, can be used [21]. These methods have to be used with care, though, when there is the possibility of self-annealing due to strong local heating during operation.

4.2. Examples for radiation effects in applications

A few typical examples will be given here for the various effects caused by ionizing radiation. Many of these examples are taken from the records of the 'Annual International Nuclear and Space Radiation Effects (NSREC)' Conferences and the 'Radiation and its Effects on Components and Systems (RADECS)' Conferences [22]. A review on terrestrial cosmic rays and SEUs caused by these is given in [23].

4.2.1. Detectors in high-dosage environment

The SMS Tracker experiment at CERN will contain 200 m² of silicon detectors [24]. These detectors are expected to survive a total flux of $3 \cdot 10^{15}$ high-energy particles per cm² over a period of 10 years. It was shown that this task can probably be achieved, though with rather unusual consequences for the devices. For tests the detectors were produced from very low n-doped wafers 300 μm thick with n- and p-diffusions on either side, respectively. The final devices will be operated at 600 V. The main concern during the operation of these devices will be the change in doping level due to the formation of divacancy-oxygen centers and the concurrent increase in dark current.

Fig. 7 depicts results showing the change of effective doping depending on the dose of 24 GeV protons and on the carbon and oxygen content of the bulk material. The 'carbonated' silicon had a carbon content of approximately $2 \cdot 10^{16}$ cm⁻³ whereas the 'oxygenated' silicon had an oxygen content of approximately $3 \cdot 10^{17}$ cm⁻³. At a dose of approximately $0,7 \cdot 10^{14}$ protons/cm² the effective doping of the bulk material changes from n-type to p-type. Fig. 7 also shows the voltage V_{Dep} necessary to have the entire 300 μm wide bulk region depleted. High oxygen content shifts the equilibrium from $V_2O + O$ to $2VO$, i.e. from doping to recombination centers, and in this way makes the devices less sensitive. When the bulk resistivity goes from n-type to p-type the junction moves from one side of the wafer to the other. Since these detectors are

intended for high-energy particle measurements, this shift apparently does not affect the operation.

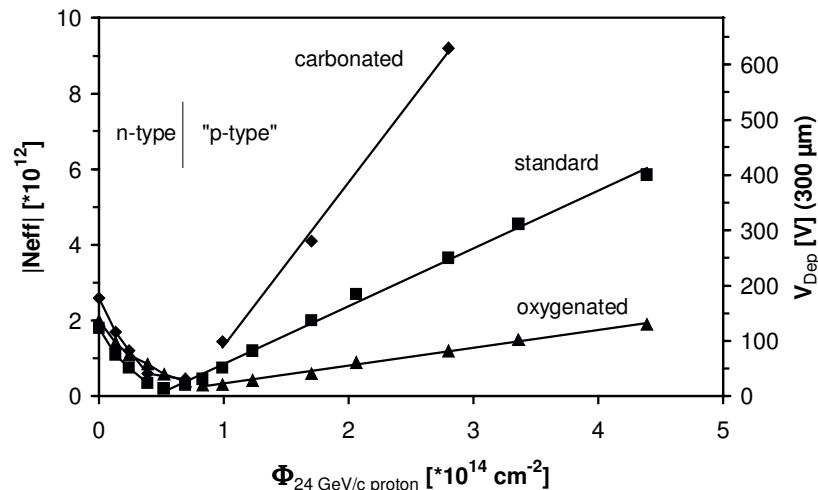


Fig. 7 Dependence of acceptor generation on proton dosage and bulk doping. V_{Dep} is the voltage necessary to expand the space charge region across the 300 μm width of the bulk region [24].

In contrast to the results in Fig. 7, the dark current does not show any dependence on bulk impurities. It depends only on the energy of the particles used and on whether particle energy generates only point defects or suffices to generate defects in clusters. In the latter case there is a linear dependence on dosage [5]. Gamma rays and low energy electrons generate only point defects leading to a dark current lower by two orders of magnitude. In the transition region there is seemingly a quadratic dependence on dosage [5].

4.2.2. Memory cells (DRAMs and SRAMs)

In DRAMs the information is stored as charge in a capacitor cell. Since the capacitor discharges with time the charge has to be replenished in regular cycles. Critical for these cells therefore is the amount of stored charge and the retention time. An ionizing event can upset the charge state of the cell and the damage occurring alongside can reduce the retention time, possibly to the point where it falls below the replenishing time (stuck bit [25]).

The sensitivity of a cell is defined in terms of a critical charge or in terms of a cross section in dependence on the energy transfer (LET) of various particles or on energy of one type particle. Fig. 8a and Fig. 8b are examples plots of such dependencies. Fig 8a depicts a typical behavior [26]. The upset cross section rises steeply beyond a minimum energy transfer and saturates at high LETs. The threshold of the LET depends on the operating voltage, but, e.g., also on the angle of incidence. In this particular device the threshold is so high that this device is insensitive to alpha particles (compare Fig. 1).

As the size of DRAM cells is steadily decreased with every new generation, there is a general tendency for the cells to become more sensitive to upsets. However, device designers have become aware of the problem and changes in the layout of the cells have compensated this trend. Fig. 8b shows for three different types of 16 MB-DRAMs a plot of the upset cross section versus proton energy [27].

SRAM memory cells are of flip-flop design having two stable states. In SRAMs SEU is influenced by the generated charge as well as by the shape of the resulting current pulse [28]. Operating conditions can be very critical. The high sensitivity of some SRAMs to the operating voltage (Fig. 9) has led to the proposal to use groups of such SRAMs in space as coarse multichannel devices detecting different threshold LETs according to their operation voltage

settings [29]. Such arrangement would have the advantage that they would not suffer from the pulse pileup problems that normal surface barrier detectors may encounter.

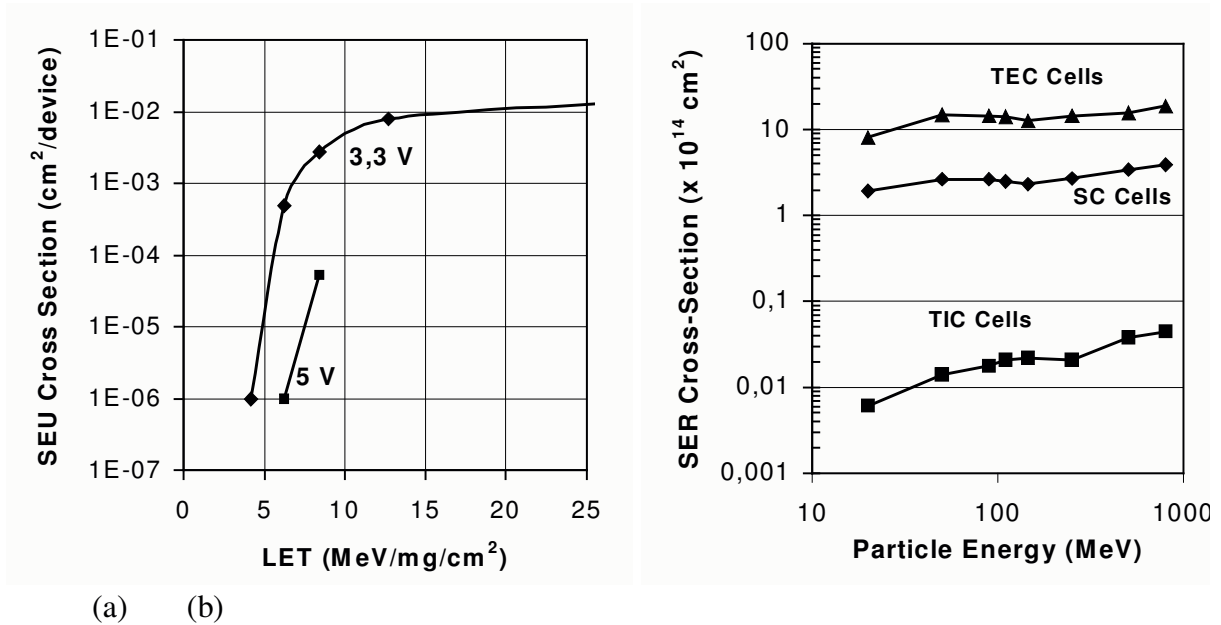


Fig. 8 (a) DRAM Single Event Upset cross section versus particle energy transfer [26]
 (b) SEU cross section for different types of 16 MB-DRAMs versus proton energy [27]

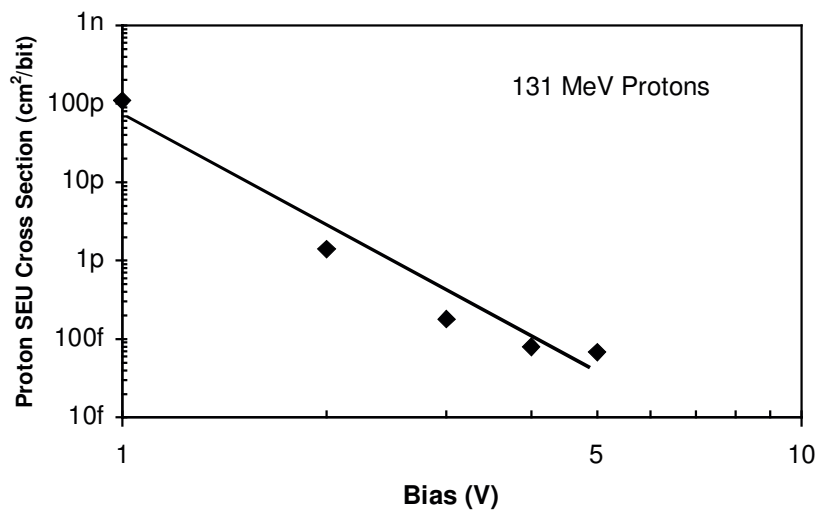


Fig. 9 SEU cross section versus bias for 256 k SRAM exposed to protons, from [28]

4.2.3. Pacemakers

Pacemakers and defibrillators deserve special attention, because with these one wants to make absolutely sure that no detrimental effects can occur due to a malfunction of the electronics. There are two settings to be investigated, the normal radiation background at ground level and at airplane cruising elevations and the increased radiation levels encountered during cancer therapy. In cancer therapy gamma rays or electron radiation are predominantly used. Hence, one has to deal with a total dose effect in this case. As miniaturization has progressed, the safe limit of some devices has fallen to 2 Gy (1 Gy = 1 J/kg) which is below the maximum therapeutic dose [30].

An extensive study of almost 600 implantable cardiac defibrillators in which any SEU of the critical SRAMs due to cosmic rays was recorded and corrected in a one-hour cycle revealed 22 upsets corresponding to a failure rate per device of approximately 100 fit, i.e. to one failure in 35

years [31] (fit stands for 'failure in time'; 1 fit corresponds to one failure in 10^9 hours). One goal of this investigation was to develop the tools to predict such low upset rates.

4.2.4. Power diodes and large-area detectors

When the high-speed train system was put into operation in Germany in 1991, it became obvious that diodes and gate-turn-off thyristors in the inverter systems of the engines failed catastrophically due to avalanche multiplication initiated by cosmic rays, i.e. by neutrons and protons (compare Fig. 5b). The burnout currents in these systems reached 100 kA. The cause was not immediately evident, because the failures occurred at voltage levels of about half the rated voltage [32]. At about the same time, similar failures were observed when high-voltage detectors were tested in particle beams [33]. In the meantime it has become clear that this type of failure limits the use of high-voltage devices in many applications even at ground level. The failure rate is extremely voltage dependent. In Fig.10 an example is given for a diode with a rated voltage of 4500 V. Not every multiplication event leads to destruction [34]. Non-destructive events were measured in a fashion as indicated in Fig. 12 with charge multiplication factors of 10^4 . When burnout occurred it happened within 100 ns after the onset of multiplication [34]. Burnout cannot be prevented in these large devices through external means, because the internal capacitance stores sufficient energy for the destruction.

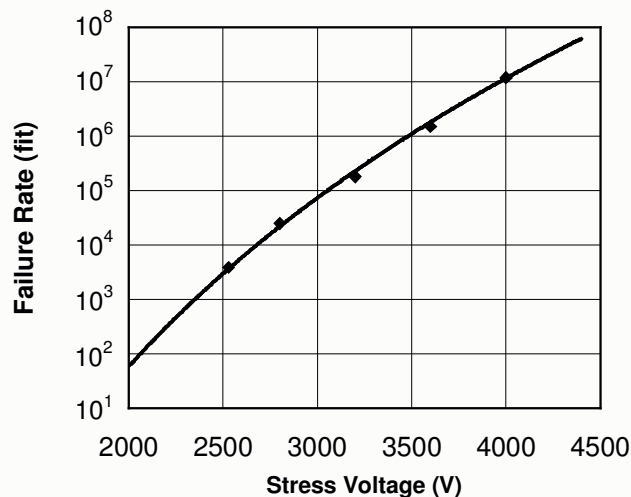


Fig. 10 Cosmic ray initiated failure rate of 4500 V power diode versus voltage [32]

4.2.5. Bipolar transistors and vertical MOSFETs

Bipolar transistors and power MOS field effect transistors are seemingly quite different devices, because during normal operation MOSFETs-transistors are unipolar. However, when it comes to SEUs these devices exhibit similar behavior, because the failure of MOS-transistors is often due to a parasitic transistor.

Fig. 11 depicts a crosscut through a power MOSFET. The parasitic transistor is formed by the $n^+ - p - n - n^+$ layers. MOSFETs may also fail due to gate rupture. This is more likely when the ion hits the device in the gate area, whereas the transistor type failure may be dominant when the device is hit in or outside of the the gate area. The transistor-type failure is a typical second breakdown event, i.e. the current generated by the absorbed ion is amplified by the transistor to a level that the blocking voltage can no longer be sustained. Typical for this type of failure is a breakdown delay of the order of a microsecond. Burnout can be prevented during testing by external current limiting or by a fast turn-off of the external circuit.

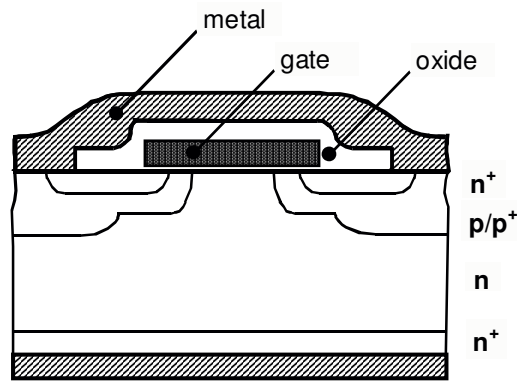


Fig. 11 Crosscut through power MOSFET

A typical behavior of a power MOSFET irradiated with nickel ions at different voltage levels is shown in Fig. 12. The device is operated like a detector [35]. At low voltage only the primary signal is recorded. As the voltage is increased an amplified signal appears. The first peak may shift due to some multiplication. If the voltage is further increased, the amplified signal reaches a critical level Q_{th} where burnout occurs, resulting in a large SEB signal.

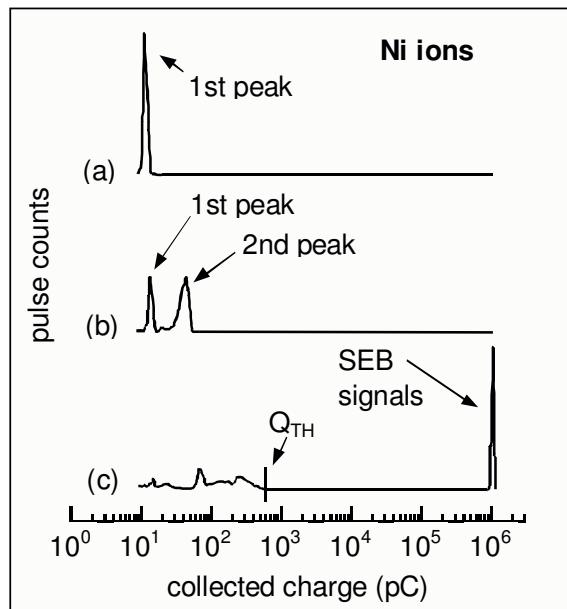


Fig. 12 Generated charge in a power MOSFET at increasing voltage levels [35]

Gate rupture seems to be more of a problem for low-voltage MOSFETs. Fig 13 depicts a collection of data from [36]. The thickness of the n-type epitaxial layer of these power MOSFETs was approximately $7 \mu\text{m}$. The minimum range of the ions used for the irradiations was $28 \mu\text{m}$. In the case of the gold ions the ionization of the n-layer was obviously so strong that the space charge layer could no longer be supported (compare Fig. 4). The maximum voltage supported by the gate oxide went down to about half its original value independent of the oxide thickness. The influence of the protons is due to short-range secondary nuclei, mostly lighter than silicon, generated in nuclear reactions. Thus the results fit well into the general scheme.

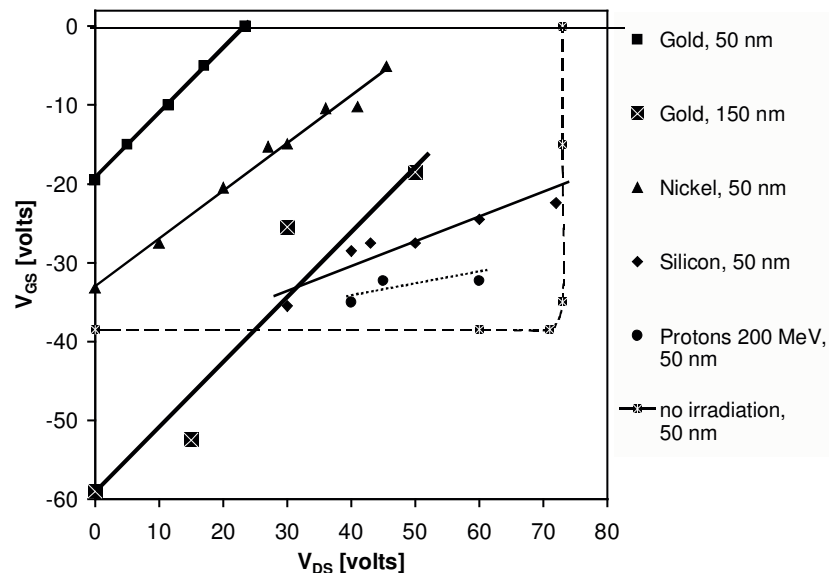


Fig. 13 Gate rupture in 60 V- MOSFETs with 50 nm and 150 nm gate oxide thickness. Variation of gate and drain voltage as well as of the ions used for irradiation. Selected from [36].

5. References

- [1] J.F. Ziegler, J.P. Biersack, U. Littmark, "The Stopping and Range of Ions in Solids", Pergamon Press, 1985
- [2] J.F. Ziegler, J.P. Biersack, "SRIM/TRIM, The Stopping and Range of Ions in Matter/ The Transport of Ions in Matter", <http://www.srim.org>, 1998
- [3] B.C. MacEvoy, "Defect Evolution in Silicon Detector Material", Nucl. Instr. Meth. Phys. Res., A 3888, 1997, 365-369
- [4] B.J. Baliga, Power Semiconductor Devices, PWS Publishing Company, 1995
- [5] J.R. Srour, D.H. Lo, "Universal Damage Factor for Radiation-Induced Dark Current in Silicon Devices", IEEE Transact. Nucl. Sci. 47, 2000, 2451-2459
- [6] S.J. Watts, J. Matheson, I.H. Hopkins-Bond, A. Holmes-Siedle, A. Mohammadzadeh, R. Pace, "A new model for generation-recombination in silicon depletion regions after neutron irradiation", Transact. Nucl. Sci. 43, 1996, 2587-2594
- [7] W. Wondrak, "Erzeugung von Strahlenschäden in Silizium durch hochenergetische Elektronen und Protonen", Dissertation, Universität Frankfurt/M, 1985
- [8] R.O. Carlson, Y.S. Sun, H.B. Assalit, "Lifetime Control in Silicon Power Devices by Electron or Gamma Irradiation", IEEE Transact. Electr. Dev. ED-24, 1977, 1103-1108
- [9] H.H.K. Tang, "Nuclear physics of cosmic ray interaction with semiconductor materials: Particle-induced soft errors from a physicist's perspective", IBM J. Res. Devel. 40, 1996, 91-108
- [10] G.R. Srinivasan, H.K. Tang, P.C. Murley, "Parameter-Free, Predictive Modeling of Single Event Upsets Due to Protons, Neutrons, and Pions in Terrestrial Cosmic Rays", IEEE Transact. Nucl. Sci. 41, 1994, 2063-2070
- [11] C.M. Hsieh, P.C. Murley, R.R. O'Brien, "A Field-funneling Effect on the Collection of Alpha-Particle-Generated Carriers in Silicon Devices", IEEE Electr. Dev. Let. EDL-2, 1981, 103-105
- [12] D. Binder, E.C. Smith, A. B. Holman, "Satellite Anomalies from Galactic Cosmic Rays", IEEE Transact. Nucl. Sci. 22, 1975, 2675-2680
- [13] T.C. May, M.H. Woods, "Alpha-Particle-Induced Soft Errors in Dynamic Memories", Transact. Electr. Dev. ED-29, 1979, 2-9
- [14] J.F. Ziegler, "Terrestrial cosmic rays", IBM J. Res. Devel. 40, 1996, 19-39

- [15] J.C. Pickel, "Single-Event Effects Rate Prediction", IEEE Transact. Nucl. Sci. 43, 1996, 483-495
- [16] E.L. Petersen, "Approaches to Proton Single-Event Rate Calculations", IEEE Transact. Nucl. Sci. 43, 1996, 496-504
- [17] P.C. Murley, G.R. Srinivasan, "Soft-error Monte Carlo modeling program, SEMM", IBM J. Res. Devel. 40, 1996, 109-118
- [18] "Particle Accelerators Around the World", http://www-elsa.physik.uni-bonn.de/Informationen/accelerator_list.html
- [19] P. Rai-Choudhury, J. Bartko, J.E. Johnson, "Electron Irradiation Induced Recombination Centers in Silicon – Minority Carrier Lifetime Control", IEEE Transact. Electr. Dev., ED-23, 1976, 814-818
- [20] J. Vobecký, P. Hazdra, J. Homola, "Optimization of Power Diode Characteristics by Means of Ion Irradiation", IEEE Transact. Electr. Dev. 43, 1996, 2283-2289
- [21] F.-J. Niedernostheide, H.-J. Schulze, U. Kellner-Werdehausen, A. Frohnmeyer, G. Wachutka, "Radiation-Induced Defects Utilized for Performance Tailoring in High-Power Devices", DECON 2001, Electrochem. Soc. Proc. Vol. 2001-29, 2001, 112-120
- [22] Records of NSREC are published in 'IEEE Transactions on Nuclear Science', those of RADECS in the IEEE Conference Records.
- [23] Special issue "Terrestrial cosmic rays and soft errors", IBM Journ. Res. Devel. 40, 1996
- [24] G. Lindström et al. , "Radiation Hard Silicon Detectors - Developments by the RD48 (ROSE) Collaboration", Intern. Symp. Dev. Appl. Semicond. Tracking Detectors", Hiroshima, 2000, Nucl. Instr. & Meth. in Phys. Res. A 466, 2001, 308-326
- [25] L.Z. Scheick, S.M. Guertin, G.M. Swift, "Analysis of Radiation Effects on Individual DRAM Cells", IEEE Transact. Nucl. Sci. 47, 2000, 2534-2545
- [26] S. Duzellier, R. Ecoffet, "Recent Trends in Single-Event Effect Ground Testing", Transact. Nucl. Sci. 43, 1996, 671-676
- [27] J.F. Ziegler, M.E. Nelson, J.D. Shell, R.J. Peterson, C.J. Gelderloos, H.P. Muhlfeld, C.J. Montrose, "Cosmic Ray Soft Error Rates of 16-Mb Memory Chips", IEEE Journ. Solid-State Circ. 33, 1998, 246-252
- [28] L.B. Freeman, "Critical charge calculations for a bipolar SRAM array", IBM J. Res. Devel. 40, 1996, 119-129
- [29] P.J. McNulty, L.Z. Scheick, S. Yow, A.B. Campbell, M.W. Savage, "Single-Chip Dosimeters to Accompany Photometric Systems Flown in Space", IEEE Transact. Nucl. Sci., 48, 2001, 2039-2042
- [30] J. Mouton, R. Trochet, J. Vicrey, M. Sauvage, B. Chauvenet, A. Ostrovski, E. Leroy, R. Haug, B. Dodinot, F. Joffre, "Electromagnetic and Radiation Environment Effects on Pacemakers" RADECS 99, IEEE Conf. Rec. 2000, 34-38
- [31] P.D. Bradley, E. Normand, "Single Event Upsets in Implantable Cardioverter Defibrillators", IEEE Transact. Nucl. Sci. 45, 1998, 2929-2940
- [32] H. Kabza, H.-J. Schulze, Y. Gerstenmaier, P. Voss, J. Wilhelmi, W. Schmid, F. Pfirsch, K. Platzöder, "Cosmic Radiation as a Cause for Power Device Failure and Possible Countermeasures", IEEE Proc. 6th Internat. Symp. Power Semicond. Devices & ICs, Davos, CH, 1994, 9-12
- [33] G. Anzivino, J. Bai, B. Benschke, A. Contin, R. DeSalvo, S. Fagen, H. He, L. Lui, M. Lundin, R.M. Madden, M.R. Mondardini, M. Swazlowski, K. Wang, X. Xia, C. Yang, M. Zhao, "Failure modes of large surface avalanche photo diodes in high-energy physics environments", Nucl. Instr. Meth. Phys. Res. A 430, 1999, 100-109
- [34] G. Soelkner, P. Voss, W. Kaindl, G. Wachutka, H.K. Maier, H.-W. Becker, "Charge Carrier Avalanche Multiplication in High-Voltage Diodes Triggered by Ionizing Radiation", IEEE Transact. Nucl. Sci., 47, 2000, 2365-2372
- [35] S. Kuboyama, S. Matsuda, T. Kano, T. Ishii, "Mechanism for Single-Event Burnout of Power MOSFETS and Its Characterization Technique", IEEE Transact. Nucl. Sc., 39, 1992, 1698-1703

- [36] J.L. Titus, C.F.Wheatley, "Proton-Induced Dielectric Breakdown of Power MOSFETs",
Transact. Nucl. Sci. 45, 1998, 2891-2897